In-Vivo Implant Mechanics of Flexible, Silicon-Based ACREO Microelectrode Arrays in Rat Cerebral Cortex

Winnie Jensen, Ken Yoshida, and Ulrich G. Hofmann

***Abstract*—The mechanical behavior of an electrode during implantation into neural tissue can have a profound effect on the neural connections and signaling that takes place within the tissue. The objective of the present work was to investigate the *in vivo* implant mechanics of flexible, silicon-based *ACREO* microelectrode arrays recently developed by the VSAMUEL consortium (European Union, grant #IST-1999-10073). We have previously reported on both the electrical [1]–[4] and mechanical [5], [6] properties of the *ACREO* electrodes. In this paper, the tension and compression forces were measured during a series of *in vivo* electrode insertions into the cerebral cortex of rats (7 acute experiments, 2-mm implant depth, 2-mm/s insertion velocity). We compared the *ACREO* silicon electrodes (4° opening angle, 1–8 shafts) to single-shaft tungsten electrodes (3° and 10° opening angles). The penetration force and dimpling increased with the cross-sectional area (statistical difference between the largest and the smallest electrode) and with the number of shafts (no statistical difference). We consistently observed tension (drag) forces during the retraction phase, which indicates that tissue sticks to the electrode within a short time period. Cleaning the electrodes prior to insertion with silane (hydrophobic) or piranha (hydrophilic) significantly decreased the penetration force. In conclusion, our findings suggest that reusable electrodes for acute animal experiments must not only be strong enough to survive a maximal force that exceeded the penetration force, but must also be able to withstand high tension forces during retraction. Careful cleaning is not only important to avoid foreign body response, but can also reduce the stress applied to the electrode while penetrating the brain tissue.**

***Index Terms*—Cerebral cortex, implant mechanics, rat, silicon electrode, tungsten electrode.**

I. Introduction

With major developments in micro-fabrication technology in recent decades, silicon-based neural prosthetic interfaces have received a great deal of attention within the fields of basic neuroscience research and rehabilitation engineering. Their ability to simultaneously record activity from many individual cells has been one of the main techniques to understand how the brain processes information to sense and control body functions. Today, such intracortical brain recordings are routinely obtained. The focus of the present work was to report on ongoing evaluation of a flexible, silicon-based electrode developed by the **VSAMUEL** consortium [European Union (EU) fifth framework, grant number IST-1999-10 073] that one day may provide an alternative interface for chronic brain implants [7]–[9]. The silicon electrode arrays were manufactured at ACREO AB, Kista, Sweden, and consisted of up to 64 channels distributed on 1–8 shafts [2]. The electrodes will be referred to as *ACREO* electrodes in the present work.

Since the use of lithographic techniques and silicon etching technology was first suggested to produce biosensors [10], [11], significant progress on biosensors for cortical implants has been made, especially with the development of batch-fabricated thin-film microelectrodes at the University of Michigan, Ann Arbor, (see, e.g., [12]) and the Utah intracortical electrode array (see, e.g., [13]). The Michigan electrodes consist of a three-dimensional (3-D) assembly of two-dimensional micro patterned silicon substrates that are used as carriers for thin-film electrodes, and these electrodes have undergone substantial mechanical evaluation and electrical recording evaluation, see, e.g., [12], and [14]–[16]. The Utah electrode is a 3-D silicon structure consisting of 100 penetrating electrodes. The long-term chronic intracortical recording and stimulation capabilities of the Utah electrode have, e.g., been demonstrated in the cat sensory cortex [17], [18].

Subdural implantation is always a traumatic intervention, and the trauma can include tearing, cutting, stretching, or compression of the tissue as an electrode is implanted or explanted, or it may result in disruption of support cells, blood vessels and neuronal processes. The cell damage may be limited if the insertion of an electrode does not result in stretching or compression of the surrounding tissue [19]. Clearly, the mechanical behavior of an electrode during implantation into neural tissue can have a profound effect on the neural connections and signaling that takes place within the tissue.

Careful cleaning has proved to be highly important to improve the biocompatibility on any implanted biosensor to prevent foreign body response during contact with biological tissue (see, e.g., [17] and [20]). The various membrane layers of the brain have varying degrees of hydrophilicity (i.e., water-attracting surface), and the arachnoid membrane

Manuscript received February 3, 2005; revised September 11, 2005. This work was supported in part by the European Union (EU) under Grant IST-1999-10073 and in part by the Danish National Research Foundation. *Asterisk indicates corresponding author.*

*W. Jensen is with Center for Sensory-Motor Interaction, Department of Health Science, Aalborg University, 9220 Aalborg, Denmark (e-mail: wj@hst.aau.dk).

K. Yoshida is with Center for Sensory-Motor Interaction, Department of Health Science, Aalborg University, 9220 Aalborg, Denmark (e-mail: ky@hst.aau.dk).

U. G. Hofmann is with Universität zu Lübeck, Institut für Signalverarbeitung und Prozessrechentechnik, **<City, postal code?>** Germany (e-mail: hofmann@isip.mu-luebeck.de).

Digital Object Identifier 10.1109/TBME.2006.872824

TABLE I
SPECIFICATIONS ON THE MICROELECTRODES INCLUDED IN THE STUDY. (* TUNGSTEN ROD: A-M SYSTEMS, INC. **ACREO ELECTRODES MANUFACTURED AT ACREO AB, SWEDEN). THE OPENING ANGLES FOR THE TUNGSTEN ELECTRODES WERE MEASURED FROM PICTURES TAKEN THROUGH A MICROSCOPE. THE NAMING CONVENTION ADAPTED WAS AS FOLLOWS: THE FIRST LETTER/NUMBER REFERS TO THE BASIC DESIGN TYPE, THE SECOND NUMBER REPRESENT THE NUMBER OF SHAFTS, AND THE THIRD NUMBER THE OPENING ANGLE

Electrode ID	Electrode Provider	Electrode Type	Number of shafts	Distance Between shafts [μm]	Opening angle [°]	Shaft size at tip [μm]	Shaft size at base [μm]	Shaft Shape	Coating	Material	Num Insertions
K1.1.4	*ACREO***	K1	1	-	4	25 x 38	25 x 200	Rectangular	Silicon Nitride (SN)	Silicon	5
K1.2.4	*ACREO***	K1	2	500	4	25 x 38	25 x 200	Rectangular	SN	Silicon	9
K1.3.4	*ACREO***	K1	3	500	4	25 x 38	25 x 200	Rectangular	SN	Silicon	10
K1.4.4	*ACREO***	K1	4	500	4	25 x 38	25 x 200	Rectangular	SN	Silicon	9
E5.8.4	*ACREO***	E5	8	200	4	25 x 38	25 x 200	Rectangular	SN	Silicon	11
M4.4.4	*ACREO***	M4	4	600	4	25 x 38	25 x 200	Rectangular	SN	Silicon	8
T1.1.3	Tungsten*	T1	1	-	4	Ø = 50	Ø = 50	Round	None	Tungsten	20
T1.1.10	Tungsten*	T1	1	-	10	Ø = 50	Ø = 50	Round	None	Tungsten	5
F1.1.10	Tungsten*	F1	1	-	10	Ø = 150	Ø = 150	Round	None	Tungsten	11

is usually impermeable to hydrophilic substances. Modifying the electrode surface properties toward hydrophilic and/or hydrophobic (i.e., water-shredding surface) states may, therefore, have an effect on the electrode insertion mechanics.

The objective of the present work was to investigate aspects of the *in vivo* implant mechanics of the flexible, silicon-based *ACREO* microelectrode arrays in comparison to conventional tungsten micro-wire electrodes. The analysis included: 1) A series of *in vivo* insertions and retractions in rat cerebral cortex, where a high-resolution load cell was used to measure tension and compression forces during the implantation process; 2) A comparison of cleaned and uncleaned off-the shelf electrodes to examine the effect of surface energy (treated with either piranha to produce a hydrophilic surface or silane to produce a hydrophobic surface).

In the present paper we present novel *in vivo* insertion force data from flexible, silicon-based electrodes into brain tissue, which will form a broad base for future electrode design and implant methodology..

II. METHODS

A. Acute Rat Preparation

Approval for all experimental procedures was obtained from the Danish Committee for the Ethical Use of Animals in Research. Data were collected from 7 acute experiments using adult Wistar rats (M/F, approximate weight of 400 g). The rats were anaesthetized using intramuscular injections Ketamine (100 mg/kg), Xylazine (5 mg/kg), and Acepromazine (2.5 mg/kg). The anesthesia was regulated by continuously monitoring the heart rate, the blood oxygen saturation and body temperature. The rat's head was anchored in a stereotaxic frame (Narishige Co., LTD, Japan). A craniectomy was performed over the somatosensory cortex area (+2 mm to +4 mm lateral and +2 mm to +4 mm caudal relative to Bregma) over the right hemisphere of the brain. The dura layer was manually retracted to expose the **<Au: Define pia?>** (pia) surface, which was continuously covered with artificial cerebral spinal fluid (130 mM NaCl, 26 mM $NaHCO_3$, 1.2 mM NaH_2PO_4, 5 mM KCl, 1.5 mM $CaCl_2$, and 2.2 mM $MgSO_4$). The cerebral cortex was chosen as the implant target, since this is the area from which we aim to record from in the future, and the cerebral cortex thickness does not vary much between mammalian species [2]. An insertion depth of 2 mm was chosen because the main target of sensory information arriving from the thalamus is located in layer IV, located at a depth of approximately 2–4 mm from the pia surface in the rat [21].

B. Description of the Electrodes and Cleaning Procedures

We compared the implant mechanics of single and multiple shafted *ACREO* electrodes with conventional single shaft tungsten electrodes (descriptive data are provided in Table I). Commercially available round tungsten rods (50 μm diameter) were cut into appropriate lengths and manually electro-sharpened. To create the tip, one end was lowered into a 2N KNO_3 solution and ac current was passed through the solution to electrolytically oxidize and etch the tip of the wire (80 V for approximately 20 s to 40 s). The tips were visually inspected, the opening angle was measured, and the electrodes were finally carefully cleaned in deionized water before implantation.

The *ACREO* electrodes were manufactured on silicon-on-insulator substrates using step-and-repeat projection lithography and reactive ion etching methods to form the electrode sites and the conductor traces. The details of the manufacturing processes are described in detail in [9]. The electrodes consisted of 1 to 8 parallel shafts [see Fig. 1(A)] with a cross-sectional area of 25 μm × 38 μm [measure "w" in Fig. 1(B)] at the electrode site. The area expanded to 25 μm × 200 μm at the shaft base. The distance between the individual shafts ranged between 200 μm and 600 μm [measure "b" in Fig. 1(B)] and each shaft had a tip opening angle of 4°. The distance between the active sites [measure "a" in Fig. 1(B)] was dependent on the total number of active sites on the individual electrode. The electrode base section had pads on it suitable for wire bonding. Each of the shafts carried a number of 10 μm × 10 μm platinum-iridium recording sites [see Fig. 1(C)]. The naming convention adapted for the different *ACREO* electrodes were based on their designs, see Table I. For example, in "K1.1.4" the first letter/number combination refers to the basic design type (assigned by the consortium), the second number represent the number of shafts, and the third number represents the opening angle.

To examine the effect of cleaning on the implant mechanics, the electrodes were cleaned using either a Piranha solution (3:1 solution of concentrated sulphuric acid (H_2SO_4) and hydrogen

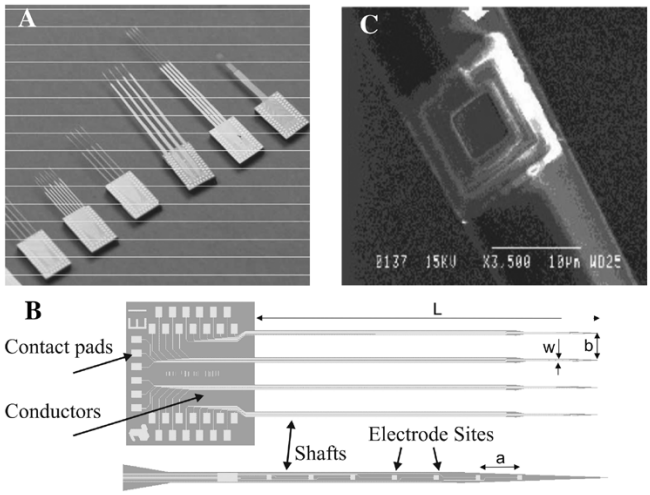

Fig. 1. (A) Examples of different ACREO electrode designs. (B) Schematic drawing of an ACREO electrode. The following parameters were used to characterize the individual electrodes: l = length of shafts, b = width between shafts, w = width of shaft at electrode site, a = distance between electrode sites. Specific information on the individual electrodes is given in Table I. (C) Close up of a single active site.

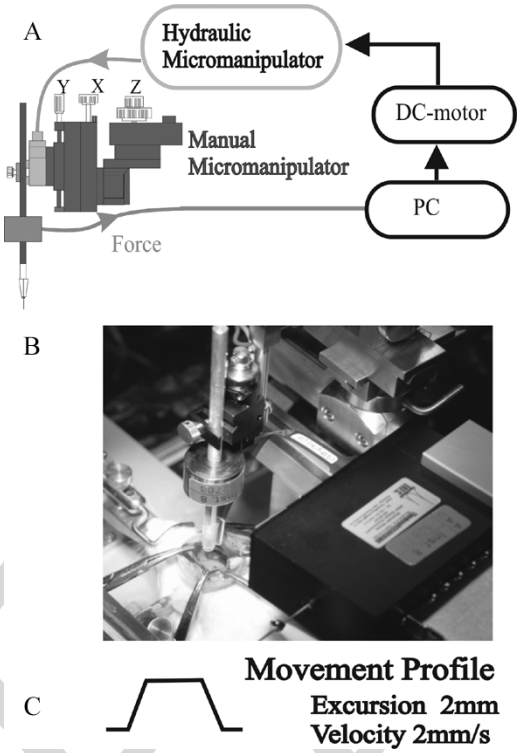

Fig. 2. Experimental setup. (A) Schematic drawing of the setup including two micromanipulators, motor and PC. (B) An electrode is seen mounted in a Luer lock that is connected to the micromanipulator. (C) The movement profile used to insert and retract electrodes into the brain tissue.

peroxide (H_2O_2) or probes were silanized by brief exposure to Dimethylsilane vapors []. These are commonly used method to clean silicon-based materials, and it removes both organic and metal residues. All electrodes were thoroughly rinsed in deionizied water before implantation.

C. Measurements and Data Analysis

Simultaneous measurements were made of the force and the distance traveled by the electrode during repeated penetration and retraction into the cerebral cortex. The experimental setup is depicted in Fig. 2(A) and Fig. 2(B). The tension and compression forces were measured using a load cell (Sensotec Inc., Model 31/1435-02, $\max.\ \text{load} = 0.1\ \text{kg}$, $\text{resolution} = 1.31\ \text{mV/g}$). A male fitting on the load cell was used to accept a female Luer lock (from a disposable hypodermic needle) onto which the electrodes were mounted. The electrode tips were placed just above and normal to the pia surface using a manually operated 3-D-micromanipulator (Fine Science Tools, MM-33). The electrodes were then advanced into the brain tissue by a motor-controlled (Maxon DC Motor 22-60-881, JVL Industri Elektronik A/S, DK) hydraulic micromanipulator (Narishige MMO-220) with a resulting movement resolution of 0.25 μm. The microelectrodes were always inserted according to a ramp-and-hold profile [$\text{velocity} = 2\ \text{mm/s}$, $\text{excursion} = 2\ \text{mm}$, see Fig. 2(C)]. The ramp-and-hold insertion was repeated twice at the same position, before the electrode was moved to a new position. The force and position signals were filtered before sampling (first-order analog filter, $\text{sampling frequency} = 2.5\ \text{kHz}$, NI DAQCard-6204E). The sampled data were filtered offline (Butterworth lowpass filters at 25 Hz for the force data and 10 Hz for the length), and any linear drift was removed after before analyses were performed.

A typical example set of measured force and length data is shown in Fig. 3. By convention for this study, compression was defined as positive force and tension was defined as negative force. The *dimpling* of the brain surface was defined as the distance traveled by the microelectrode from the beginning of the insertion (electrode placed right at 0 mm at the surface of the brain) to the point of penetration, see Fig. 3(A), (B). The *point of penetration* was defined as the first peak in the force curve [Fig. 3(B)] or in the corresponding length/force curve [Fig. 3(C)]. At 2 mm the electrode was fully advanced into the cerebral cortex. We typically observed a simultaneous increase in the force and dimpling (i.e., compression of the brain tissue) until the point of penetration, where after the force abruptly decreased and the dimpling disappeared. If this typical behavior was observed, it was taken as evidence that the electrode had actually penetrated the pia surface and at this point the *penetration force* was determined. We verified this through visual inspection of the electrode and brain movements during the actual experiment and by carefully evaluating and comparing the force and length data with the visual observations. The *maximum compression force* experienced by the electrode during an entire insertion-retraction phase was determined. The minimal compression force, when the electrode was fully advanced into the brain, which is also referred to as the *rest force*. Finally, we determined the maximal tension force experienced by the electrode during the retraction phase, referred to as the *drag*

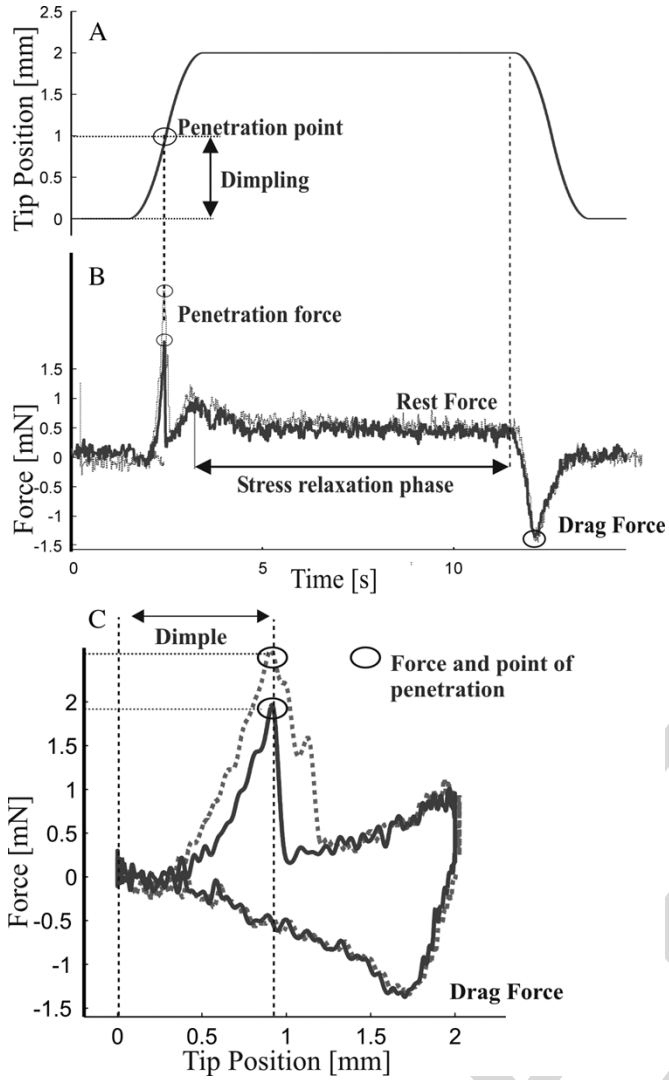

Fig. 3. Typical measurement taken during insertion of a single shaft silicon electrode into rat cerebral cortex. The dashed, light grey curves correspond to the first insertion-retraction phase, whereas the solid, dark grey curves represent the second insertion. (A) Position of the electrode while advancing it into the brain. At 0 mm the electrode is at the surface of the brain and at 2 mm the electrode is fully advanced into the brain. (B) Force traces. The dura mater was removed prior to implantation, while the pia mater was left intact. The following points of the data were compared: penetration force, rest force, drag force and dimpling. (C) Length-force curves were plotted to better identify the penetration force, the penetration point, and the drag force.

force. Statistical evaluation of the force at the selected points was performed using analysis of variance (ANOVA) with Newmann-Keuls or Turkey-Kramer post-hoc evaluation.

III. Results

A. Insertion Forces in Rat Cerebral Cortex

We evaluated and compared the force and depth of the penetration point of the single-shaft versions of the *ACREO* silicon electrodes with 50 μm and 150 μm standard tungsten electrode, see Fig. 4(A). We found that the single-shafted silicon electrode had the smallest dimple (first insertion: 0.37 ± 0.14 mm, second insertion: 0.32 ± 0.12 mm) and smallest penetration force (first insertion: 0.48 ± 0.18 mN, second insertion: 0.10 ± 0.04 mN) of all the electrodes tested. The highest penetration force among the single-shaft electrodes was found with the 150 μm diameter tungsten microelectrode during the first insertion (1.15 ± 0.51 mN), i.e., the microelectrode that had the highest cross-sectional area and the largest opening angle. There was a statistical significant difference in penetration force only between the largest tungsten electrode and the *ACREO* silicon electrode (ANOVA, Newman-Keuls post-hoc analysis, $p < 0.05$). However, a statistical significant difference in the dimple depth produced by the different types of electrodes (ANOVA, Newman-Keuls post-hoc analysis, $p < 0.05$).

We also examined the effect of the number of shafts on the penetration force during the second insertion within the group of *ACREO* electrodes, see Fig. 4(B). In order to compare results, we calculated the specific penetration force by normalizing the measured penetration force with the number of shafts of each electrode. We observed a weak general trend of a linear decrease in specific force and a correspondingly increase in dimple depth with the number of shafts. However, no statistical significant differences were found among the specific penetration forces or dimple depths (ANOVA, Newman-Keuls post-hoc analysis, $p < 0.05$).

Fig. 4(C) compares the penetration, maximum, rest and drag force of the first and second insertion for a single-shafted *ACREO* electrode, and Table II summarizes the mean and standard deviation forces for all electrodes included in the study. A significant variation was found in the initial penetration force of all electrodes that was believed to be caused by the initial rupture of the pia layer. The comparisons were, therefore, mainly limited to the data collected from the second insertion phase.

Throughout all experiments, we observed a stress relaxation phase in the time period where the electrode was fully advanced into the brain tissue. The force never reached a constant compression level or declined to zero, even in selected trials where we kept the microelectrodes inserted for a period of 30 s (the results were not included in the present dataset). The mechanism of the stress relaxation can be thought of as the redistribution of the tension through slow stretching and elongation of the tissue matrix following insertion of the foreign structure into the tissue. In the case of cortical tissue, this relaxation can take place by stretching of structural components of the neuropil and may, therefore, affect the neural processes.

During the retraction phase a tension force was generally observed. This occurrence of a tension force was used as an indication of the electrodes had penetrated the pia. We attempted in several trials to insert several types of electrodes with the dura maintained intact without success, and in these cases no tension force was observed during the retraction phase.

B. Effect of Cleaning on the Implant Mechanics

The results from evaluating the effect of cleaning the electrode on the implantation mechanics are summarized in Fig. 4(D). We observed that modifying the surface energy of the electrode by cleaning had little effect on the depth of the dimple during implantation. The smallest dimple was seen with the Piranha cleaned electrodes, while the largest dimple was seen with the Silane treated electrodes, and the uncleaned electrode had

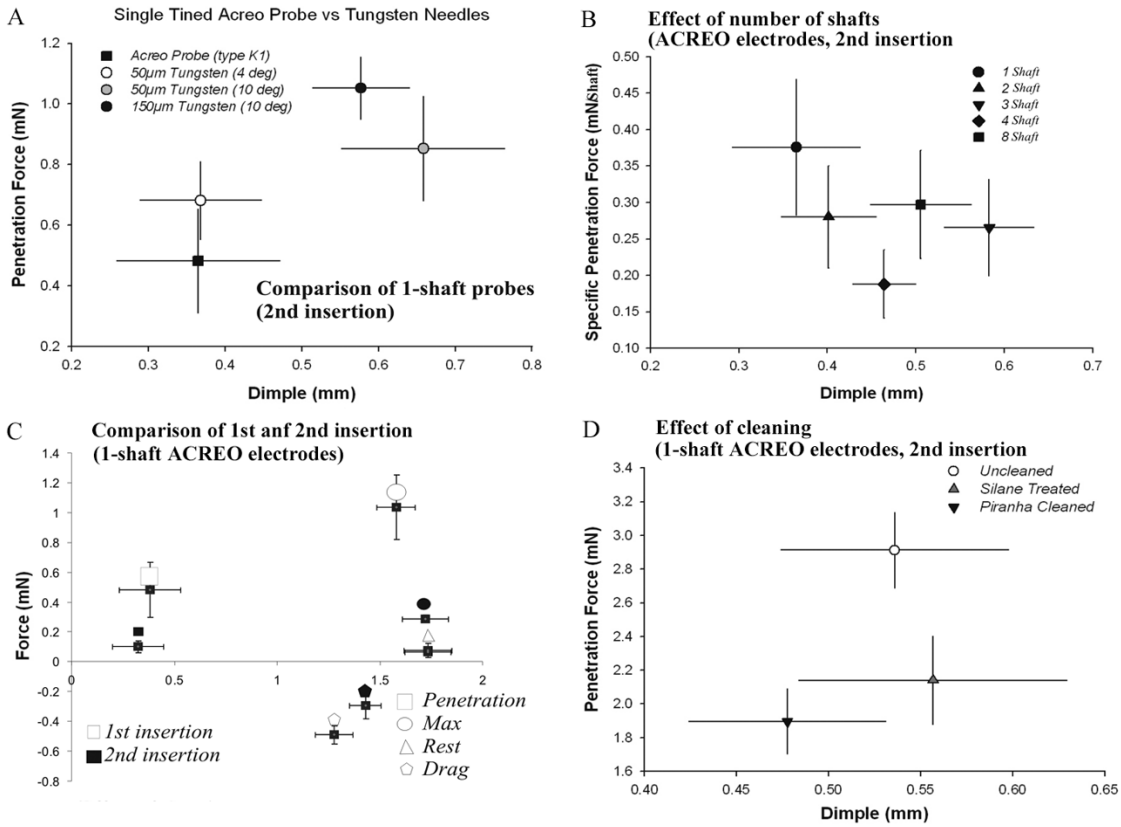

Fig. 4. (A) Comparison of penetration points for single shaft silicon electrodes with standard tungsten needle electrodes. The single shafted silicon electrode has the smallest penetration point as compared to standard tungsten needle electrodes (no statistical difference). (B) The influence of the number of shafts on a multishaft fork type silicon electrode. Multiple shafts increase the penetration force, but the specific force (force/shaft) remains constant (no statistical difference). Mean and standard deviation are shown in all plots. (C) Comparison of first and second insertion forces for single shaft silicon electrodes with standard tungsten needle electrodes (statistical difference). (D) Effect of treating the electrode surface with Silane and Piranha (statistical difference between cleaned and noncleaned electrodes).

dimple depths between the two. There were, however, no statistical significant difference in dimple depth between the group of cleaned and uncleaned electrodes (ANOVA analysis, $p < 0.05$).

The treatments reduced the penetration force and we found a statistical significant difference between the two groups of cleaned electrodes and the uncleaned electrodes. There was however no statistical significant difference in penetration force between piranha and the silane treated electrodes (ANOVA analysis, Neumann-Keuls post hoc analysis, $p < 0.05$).

IV. Discussion and Conclusions

A. Methodological Considerations

We have previously reported on preliminary insertion force measurements of a tungsten electrode in rabbit peripheral nerve [1], where we used a lateral displacement transducer attached to a spring and estimated the force using Hooke's law. This complex mechanical system has several components interacting that complicate the interpretation of the results, and the device was also limited to only measure compression forces. Also, other reports on the penetration of brain tissue only report on p[illegible] sion force data during the implant insertion phase [10], [24], [25]. In this paper, we used a highly accurate load cell to continuously measure both tension and compression forces, that allowed us to obtain data from both the implantation and retraction phases.

A low insertion velocity has the advantage of generating minimal vibration and mechanical shock to the brain while inserting electrodes [1[illegible]nd in the present work, we chose a low, fixed insertion velocity at 2 mm/s. Edell *et al.* have argued that using a high insertion velocity has the advantage of compensating for a poor tip design. F[illegible]xample, an electrode with a blunt tip/a large opening angle will not penetrate the brain easily unless if the insertion velocity is high [[illegible]]. The effect of insertion velocity on implanting the Utah electrode array into feline cortical tissue was examined by Rousche *et al.* [[illegible]]. In this case, a pneumatic device was designed to insert the 100-shaft Utah electrode array into the brain tissue to avoid elastic compression that appeared during manual insertion attempts. They found that an insertion speed of at least 8.3 m/s was necessary to drive the electrode fully to the desired depth of 1.5 mm. In recent investigations, we used a standard 3-body viscoelastic model (one elastic and one damping element in parallel with a second elastic element) to model the insertion force. These preliminary investigations show, that the stress relaxation behavior of the insertion force has an effect at frequencies less than 1 Hz, and that the viscoelastic properties of the tissue does not change at higher frequencies. The results, therefore, indicate, that there is no advantage of using higher speed or ballistic implantation compared to

TABLE II
COMPARISON OF THE MEASURED PENETRATION, MAXIMUM, REST, AND DRAG FORCES, AND THE DIMPLE AT THE POINT OF PENETRATION FOR THE DIFFERENT GROUPS OF ELECTRODES STUDIES. ALL DATA HAVE BEEN CORRECTED FOR ANY FORCE OFFSET

Electrode ID	1st insertion FORCE Mean ± std [mN]				2nd insertion FORCE mean ± std [mN]				1st insertion DIMPLE mean ± std [mm]	2nd insertion DIMPLE mean ± std [mm]
	Penetration	Max	Rest	Drag	Penetration	Max	Rest	Drag	At Penetration	At Penetration
K1.1.4	0.48±0.18	1.03±0.21	0.07±0.04	-0.49±0.06	0.10±0.04	0.29±0.02	0.07±0.02	-0.29±0.09	0.37±0.14	0.32±0.12
K1.2.4	0.86±0.36	1.08±0.19	0.22±0.05	-0.80±0.17	0.17±0.23	0.50±0.13	0.15±0.07	-0.59±0.13	0.40±0.13	0.46±0.18
K1.3.4	1.81±0.54	2.01±0.52	0.69±0.40	-1.30±0.32	0.53±0.46	1.16±0.62	0.51±0.42	-0.98±0.22	0.58±0.20	0.57±0.21
K1.4.4	0.83±0.37	1.82±0.44	0.60±0.26	-1.38±0.58	0.21±0.13	1.13±0.42	0.42±0.28	-1.15±0.49	0.37±0.14	0.33±0.12
E5.4.4	2.42±0.77	3.16±0.75	0.69±0.29	-2.06±0.58	0.23±0.15	0.96±0.34	0.48±0.31	-1.21±0.30	0.53±0.14	0.62±0.33
M4.4.4	2.04±0.77	3.79±1.23	1.42±0.51	-2.21±0.55	0.52±0.31	2.08±0.45	1.17±0.36	-1.87±0.56	0.54±0.18	0.64±0.23
T1.1.3	0.62±0.26	0.74±0.23	0.22±0.14	-0.56±0.20	0.16±0.12	0.44±0.20	0.15±0.11	-0.45±0.20	0.38±0.09	0.46±0.24
T1.1.10	0.85±0.33	0.99±0.31	0.28±0.07	-0.58±0.08	0.24±0.09	0.59±0.17	0.15±0.05	-0.46±0.19	0.58±0.20	0.56±0.25
F1.1.10	1.15±0.51	1.65±0.35	0.54±0.12	-0.89±0.11	0.10±0.05	0.66±0.18	0.28±0.10	-0.62±0.15	0.47±0.22	0.50±0.36
Mean std	**1.45±1.04**	**0.28±0.39**	**0.57±0.50**	**-1.15±0.70**	**0.28±0.39**	**0.91±0.61**	**0.40±0.43**	**-0.87±0.52**	**0.48±0.18**	**0.54±0.28**

the relatively slow ramp insertion we used in the present work. Results from this modeling have not been included in the present work and will be presented in a later publication.

B. On the Experimental Insertion Force Measurements

We observed that the penetration force and the dimpling were dependent on the cross-sectional area and the absolute penetration force increased with the number of shafts. The maximal penetration force was found for the *ACREO* electrodes with the highest number of shafts, i.e., the 5 shaft electrode (2.42 ± 0.77 mN) and the 8-shaft electrode (2.04 ± 0.77 mN). We observed an overall higher variation in the penetration force during the first insertion, and our findings suggest that the rupture of the pia membrane during the first insertion may be responsible for explaining a major part of the variation in penetration force during the first insertion. Once the pia membrane had been penetrated, the overall variation of the data decreased, and we, therefore, believe that the force measurements of the second insertion reflect the viscoelastic properties of the brain tissue.

The penetration forces observed in this study are comparable with the measured penetration force of a tungsten electrode in rat cerebral cortex by Hofmann *et al.* [ ]. However, Najafi *et al.* reported a penetration stress for Michigan microelectrodes between 4×10^8 dynes/cm^2 and 1.2×10^9 dynes/cm^2 (corresponding to 0.04 mN/μm^2 and 0.12 mN/μm^2, cross-sectional area of 900 μm^2 and 1200 μm^2, opening angle $= 60°$) when the electrodes penetrated the pia membrane in an *in vivo* rat preparation [ ]. Portillo and co-workers has reported similar results when penetrating the rat pia membrane, i.e., their penetration stress was 4×10^8 dynes/cm^2 (corresponding to 0.04 mN/μm^2, cross sectional area $= 4415$ μm^2, opening angle $= 30°$). In comparison, the maximal penetration forces for the *ACREO* electrodes were an order of magnitude *lower* than what has previously reported necessary for penetrating the rat pia membrane, i.e., 0.0025 mN/μm^2 for the 5-shaft electrode and 0.0021 mN/μm^2 for the 8-shaft electrode. The cross-sectional area of the Michigan and the *ACREO* electrodes are comparable and, therefore, the difference in opening angles of the two electrodes may explain the differences in penetration forces. This is further supported by observations by Edell *et al.* penetration of the dura was difficult with electrodes that had an opening angle larger than 40°–50°, whereas the electrodes with opening angles less than 20° could penetrate the dura without causing any dimpling [1].

When the electrodes were fully advanced into the brain, we observed a decline in compression force over time, however the compression force never decreased to zero. These findings indicate that chronically implanted electrodes experience a constant compression force while inserted in the brain, that may slowly push the electrode out of the brain with time if there is nothing to keep the electrode in a fixed position, or if the stiffness of the electrode or attached cable is too small to counteract for the constant compression force.

By introducing a force measurement technique that allowed us to measure both tension and compression forces, we were able to characterize the implant mechanics both during insertion and retraction that, to the best of our knowledge, have not previously been described in the literature. We consistently observed drag (i.e., tension forces) during the phase where the electrodes were retracted from the brain. During the first retraction the drag force was of similar size to the penetration force, however, during the second retraction the drag force was consistently higher than the penetration force (up to 6.2 times higher). The consistently high drag forces we observed indicates that brain tissue stick to the electrode within a short time period (<2 s). Brain electrodes that are re-used for acute animal experiments must, therefore, not only be strong enough to survive a maximal force that exceeds the penetration force, but it must also be able to withstand high tension forces during retraction.

We expect that the present design of the ACREO electrodes are strong and flexible enough to survive long-term implant and overcome micro-motions of the brain, however it will be necessary to evaluate these long-term issues in future work.

C. On the Importance of Cleaning on the Insertion Force Measurements

Treatment of the *ACREO* electrodes with Silane or Piranha prior to insertion showed to statistical significantly decrease

the penetration forces compared to uncleaned electrodes, however we found no significant difference in dimple depth among the three groups. Our results suggest that either cleaning or modifying the hydrophilicity/hydrophobicity of the surface by cleaning is an important factor to minimize the overall insertion force since the clean, hydrophilic surface resulted in the smallest dimpling and insertion forces measured. Though the dimple trend is not statistically significant, together, these results may suggest that two processes are at play here, where cleaning reduces the penetration forces possibly by removing contaminants that may roughen the electrode surface, while surface energy modification influences the degree of dimpling.

ACKNOWLEDGMENT

The authors would like to thank P. Norlin, *ACREO* AB, Kista, Sweden for providing the *ACREO* electrodes and pictures of electrodes used in this paper. They would also like to thank to the staff at Biomedicinsk Laboratorium, Aalborg Hospital, Aalborg, Denmark, for assistance during the animal experiments.

REFERENCES

1] G. O. Young, "Synthetic structure of industrial plastics," in *Plastics*, J. Peters, Ed., 2nd ed. New York: McGraw-Hill, 1964, vol. 3, pp. 15–64.

2] K. Yoshida, W. Jensen, P. Norlin, M. Kindlundh, and U. G. Hofmann, "Characterization of silicon microelectrodes from the EU ACREO project," in *Proc. 35. Jahrestagung der Deutschen Gesellschaft für Biomedizinische Technik (DGMBT)*, 2001, p. **<page range or location of conf.?>**.

] G. Biella, L. Uva, U. G. Hofmann, and M. de Curtis, "Associative interaction within the superficial layers of the entorhinal cortex of the guinea pig," *J. Neurophysiol.*, vol. 88, pp. 1159–1165, 2002.

] A. Volny-Luraghi, R. Maex, B. Vos, and E. de Schutter, "Peripheral stimuli excite coronal beams of golgi cells in rat cerebellar cortex," *Neuroscience*, vol. 113, no. 2, pp. 363–373, 2002.

] W. Jensen, K. Yoshida, T. Malina, and U. G. Hofmann, "Measurement of intrafascicular insertion force of a tungsten needle into peripheral nerve," in *Proc. 23rd Annu. Int. Conf. IEEE-EMBS*, 2001, vol. 3, pp. 3108–3109.

W. Jensen, U. G. Hofmann, and K. Yoshida, "Assessment of subdural insertion force of single-tine microelectrodes in rat cerebral cortex," in *Proc. 25th Annu. Int. Conf. IEEE*, , 2003, vol. 3, pp. 2168–2171.

] U. G. Hofmann, E. de Schutter, E. de Curtis, K. Yoshida, U. Thomas, and P. Norlin, "On the design of multi-site microelectrodes for neuronal recordings," in *Proc. MICROtec.*, 2000, vol. 1, pp. 283–288.

] P. Norlin, M. Kindlundh, A. Mouroux, K. Yoshida, W. Jensen, and U. G. Hofmann, "A 32-site neural recording electrode fabricated by double sided deep reactive ion etching of silicon-on-insulator substrates," *J. Micromech. Microeng.*, 2001.

] U. G. Hofmann, A. Folkers, T. Malina, G. Biella, E. de Curtis, E. de Schutter, K. Yoshida, U. Thomas, D. Höhl, and P. Norlin, "Toward a versatile system for advanced neuronal recordings using silicon multisite electrodes," *Biomedizinische Technik*, vol. 45, no. E1, pp. 169–170, 2000.

0] K. D. Wise and J. B. Angell, "A low-capacitance multielectrode for use in extracellular neurophysiology," *IEEE Trans. Biomed. Eng.*, vol. BME-22, no. 3, pp. 212–219, Mar. 1975.

1] ——, "An integrated circuit approach to extracellular microelectrodes," *IEEE Trans. Biomed. Eng.*, vol. BME-17, no. 3, pp. 238–247, Mar. 1970.

] D. J. Anderson, K. Najafi, S. J. Tanghe, D. A. Evans, K. L. Levy, J. F. Hetke, X. Xue, J. J. Zappia, and K. D. Wise, "Batch-fabricated thin-film electrodes for stimulation of the central auditory system," *IEEE Trans. Biomed. Eng.*, vol. 36, no. 7, pp. 693–704, Jul. 1989.

3] K. E. Jones, P. K. Campebell, and R. A. Normann, "A glass/silicon composite intracortical electrode array," *Ann. Biomed. Eng.*, vol. 20, pp. 423–437, 1992.

] D. R. Kipke, R. J. Vetter, J. C. Williams, and J. Hetke, "Silicon-substrate intracortical microelectrode arrays for long-term recording of neuronal spike activity in cerebral cortex," *IEEE Trans. Rehabil. Eng.*, vol. 11, no. 2, pp. 151–155, Jun. 2003.

5] R. J. Vetter, J. C. Williams, J. Hetke, E. A. Nunamaker, and D. R. Kipke, "Chronic neural recording using silicon-substrate microelectrode arrays implanted in cerebral cortex," *IEEE Trans. Biomed. Eng.*, vol. 51, no. 6, pp. 896–904, Jun. 2004.

6] K. Najafi and J. Hetke, "Strength characterization of silicon microelectrodes in neurophysiological tissues," *IEEE Trans. Biomed. Eng.*, vol. 37, no. 5, pp. 474–481, May 1990.

7] P. J. Rousche and R. A. Normann, "Chronic recording capability of the utah intracortical electrode array in cat sensory cortex," *J. Neurosci. Meth.*, vol. 82, pp. 1–15, 1998.

8] ——, "Chronic Intracortical Microstimulation (ICMS) of cat sensory cortex using the utah intracortical electrode array," *IEEE Trans. Rehabil. Eng.*, vol. 7, no. 1, pp. 56–68, Mar. 1999.

9] D. J. Edell, V. V. Toi, V. M. McNeil, and L. D. Clark, "Factors influencing the biocompatibility of insertable silicon microshafts in cerebral cortex," *IEEE Trans. Biomed. Eng.*, vol. 39, no. 6, pp. 635–643, Jun. 1992.

0] P. Heiduschka and S. Thanos, "Implantable bioelectronic interfaces for lost nerve functions," *Prog. Neurobiol.*, vol. 55, pp. 433–461, 1998.

1] E. R. Kandel, J. H. Schwartz, and T. M. Jessell, "The anatomical organization of the central nervous system," in *Principles of Neural Science*, 4th ed. New York: McGraw-Hill/Appleton & Lange, 2000, pp. 316–336.

2] F. Portillo, P. Mobley, J. Moore, and D. McCreery, "Feasibility of a central nervous system auditory prosthesis: penetrating microelectrode insertion force studies," *Ann. Otol. Rhinol. Laryngol. Suppl.*, vol. 166, pp. 31–33, 1995.

3] R. C. Ritter, E. G. Quate, G. T. Gillies, M. S. Grady, M. A. Howard, and W. C. Broaddus, "Measurement of friction on straight catheters in *in vitro* brain and phantom material," *IEEE Trans. Biomed. Eng.*, vol. 45, no. 4, pp. 476–485, Apr. 1998.

4] P. J. Rousche and R. A. Normann, "A method for pneumatically inserting an array of penetrating electrodes into cortical tissue," *Ann. Biomed. Eng.*, vol. 20, pp. 413–422, 1992.

5] U. Knopp, W. Jensen, D. T. Kewley, J. M. Bower, K. Yoshida, and U. G. Hofmann, "Compression of the cerebral cortex during corticotomy: a study of dimpling in rats," presented at the 55. A hrestagung der Deutschen Gesellschaft für Neurochirurgie, **<Loc of Conf?>**, 2004, unpublished.

Winnie Jensen received the M.Sc. in electrical engineering in 1997 and the Ph.D. degree in bioengineering in 2001 from the Department of Health Science and Technologoy, Aalborg University, Aalborg, Denmark.

She is currently affiliated with both Aalborg University and University of Illinois at Chicago as a Research Associate Professor. Her main research interests include integration of neural prosthesis applications at peripheral and cortical level, and how myopathological and neuropathological conditions affect the neural prosthesis applications.

Ken Yoshida received the B.S.E. degree in bioengineering in 1989 from the University of California at Los Angeles, and the Ph.D. degree in bioengineering from the University of Utah, Salt Lake City, in 1994.

From 1995 to 1998, he was an Alberta Heritage Foundation for Medical Research and a Canadian NeuroScience Network Postdoctoral Fellow with the Division of Neuroscienceat, University of Alberta, Edmondton, AB, Canada. He is currently an Associate Professor in the Department of Health Science and Technology at Aalborg, University, Aalborg, Denmark. His research focus is the development of selective neural interfaces, and the application of these devices to study natural neuromuscular control and to investigate natural sensor based FNS systems.

Dr. Yoshida is a member of the Society for Neuroscience, the International Functional Electrical Stimulation Society, the Biomedical Engineering Society, the IEEE Engineering in Medicine and Biology Society, and Tau Beta Pi.

Ulrich G. Hofmann received the Diploma in physics and the Ph.D. degree in biophysics from the Technical University of Munich, Munich, Germany, in 1993 and 1996, respectively. He [illegible]n EU-Fellow (HCM[illegible]e Abo Akademi, **<L[illegible]n?>**, Finland, in **<y[illegible]** and a Feodor-Lynen-Fellow at the Cali[illegible]a Institute of Technology, Pasadena, in **<ye[illegible]** Since 1999, he is Senior Researcher and group leader in neuroengineering at the Institute for Signal Processing, University of Lübeck, Lübeck, Denmark. He teaches biomedical engineering and computational neurosciences. H[illegible] is to improve invasive brain-machine interfaces.